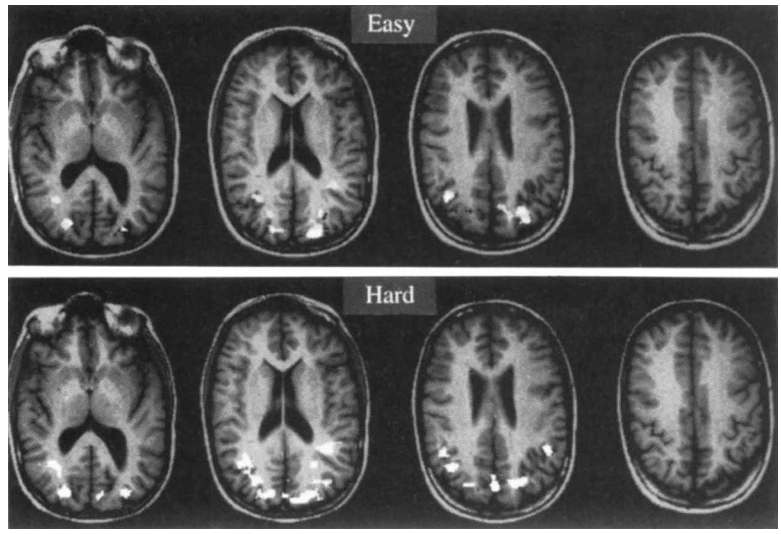

FIG. 4 Regions significantly activated in the spatial-rotation task studied with two different levels of a difficulty in a single subject. In these studies, comparison of the same spatial task used in the dual-task studies was made against a sensorimotor control task which required subjects to respond left and right alternatively to three empty squares. The task consisted of four 40-s blocks of the dot-location task alternating with four 40-s blocks of the sensorimotor control task, accumulating 160 gradient-echo echo-planar images in each activation run. Activation maps were obtained using a pixel by pixel correlation analysis to identify pixels whose signal intensity over time followed a predefined task-related reference function[22], using a threshold from $r>0.2$, $P<0.01$ (grey) to $r>0.3$, $P<0.0001$ (white); negative signal changes are not displayed. Both conditions activated identical regions in bilateral parietooccipital regions. There was greater activation (1.3% versus 0.8% signal change, $P<0.001$) and spatial extent (145 versus 89 pixels, $P<0.0001$) during the more difficult condition (left) compared to the less difficult task (right). Activation of prefrontal cortex was not observed.

inate the possibility that prefrontal cortex activation was due to a nonspecific increase in mental effort required to perform the dual task, rather than a specific type of working-memory processing, namely, a central executive system. In separate experiments, we addressed this issue by having subjects perform the spatial-rotation task alone at different levels of difficulty. Even at the more difficult condition, when performance was worse than that seen in the dual-task condition, we did not observe any prefrontal activation. We conclude that the prefrontal activation observed is related specifically to dual-task performance.

The anterior cingulate was also activated in most subjects only during the dual-task condition. Anterior cingulate activation has been observed in several cognitive neuroimaging studies[13–15], and this region has been proposed to be part of an anterior attentional system that is critical for response selection among competing, complex contingencies[16]. For example, using positron emission tomography[13], anterior cingulate as well as dorsolateral prefrontal cortex was recruited in a divided-attention task during which subjects had to detect a change in the shape, colour or speed of a visual stimulus. These regions were not recruited when subjects had to attend selectively to only one of these attributes. Simultaneous attention to multiple-stimulus attributes is analogous to performing a dual task and is likely to require the CES of working memory. Thus anterior cingulate cortex activation is also consistent with our hypothesis for the neural basis of the CES. Moreover, recruitment of anterior cingulate and dorsolateral prefrontal cortex, which are anatomically interconnected[17], suggests that the CES may comprise several components. This idea has been proposed in behavioural studies[18], and is supported by single-neuron recording experiments in non-human primates[19].

A potentially important finding in this study is the variability in the distribution of activated regions within the prefrontal cortex. This variability may reflect differing strategies used by neurologically intact subjects to perform a dual task. Investigation of other dual-task paradigms will provide additional information about the adaptive nature of distributed cognitive networks involved in working memory. Another source of variability in activation among subjects may arise from individual differences in the extent to which our dual-task paradigm placed demands on the CES. Studies that carefully monitor individual differences in available resource capacity for dual-task performance are necessary to address this issue. □

Received 8 June; accepted 7 September, 1995.

1. Baddley, A. *Working Memory* (Oxford Univ. Press, New York, 1986).
2. Petrides, M., Alivisatos, B., Meyer, E. & Evans, A. *Proc. natn. Acad. Sci. U.S.A.* **90,** 878–882 (1993).
3. Jonides, J. *et al. Nature* **363,** 623–625 (1993).
4. Cohen, J. *et al. Hum. Brain Mapp.* **1,** 293–304 (1994).
5. McCarthy, G. *et al. Proc. natn. Acad. Sci. U.S.A.* **91,** 8690–8694 (1994).
6. Swartz, B. *et al. Cereb. Cort.* **3,** 205–214 (1995).
7. Fuster, J. & Alexander, G. *Science* **173,** 652–654 (1971).
8. Goldman-Rakic, P. in *Handbook of Physiology* Vol. 5 (eds Mountcastle, V. B., Plum, F. & Geiger, S. R.) 373–417 (American Physiological Society, Bethesda, 1987).
9. Ogawa, S. *et al. Biophys. J.* **64,** 803–812 (1993).
10. Démonet, J. *et al. Brain* **115,** 1753–1768 (1992).
11. Haxby, J. *et al. Proc. natn. Acad. Sci. U.S.A.* **88,** 1621–1625 (1991).
12. D'Esposito, M. *et al. Neuropsychology* (in the press).
13. Corbetta, M., Miezin, F., Dobmeyer, S., Shulman, G. & Petersen, S. *J. Neurosc.* **11,** 2383–2402 (1991).
14. Pardo, J., Pardo, P., Janer, K. & Raichle, M. *Proc. natn. Acad. Sci. U.S.A.* **87,** 256–259 (1990).
15. Raichle, M. *et al. Cereb. Cort.* **4,** 8–26 (1994).
16. Posner, M. & Petersen, S. *A. Rev. Neurosci.* **13,** 25–42 (1990).
17. Goldman-Rakic, P. *A. Rev. Neurosci.* **11,** 137–156 (1988).
18. Van der Linden, M., Coyette, F. & Seron, X. *Cogn. Neuropsychol.* **9,** 301–326 (1992).
19. Goldman-Rakic, P., Chafee, M. & Friedman, H. in *Brain Mechanisms of Perception and Memory: From Neuron to Behavior* (eds Ono, T., Squire, L., Raichle, M., Perret, D. & Fukuda, M.) 445–456 (Oxford Univ. Press, New York, 1993).
20. Kwong, K. K. *et al. Proc. natn. Acad. Sci. U.S.A.* **89,** 5675–5679 (1992).
21. Talairach, J. & Tournaux, P. *Co-Planar Stereotaxic Atlas of the Human Brain* (Thieme, New York, 1988).
22. Bandettini, P. A., Jesmanowitz, A., Wong, E. C. & Hyde, J. S. *Magn. Reson. Med.* **30,** 161–173 (1993).

ACKNOWLEDGEMENTS. This work was supported by grants from the Charles A. Dana Foundation, the McDonnell-Pew Program in Cognitive Neuroscience, and the US Public Health Service.

Specificity of monosynaptic connections from thalamus to visual cortex

R. Clay Reid & Jose-Manuel Alonso

Laboratory of Neurobiology, The Rockefeller University, New York, New York 10021, USA

In cortical area 17 of the cat, simple receptive fields are arranged in elongated subregions that respond best to bright (on) or dark (off) oriented contours, whereas the receptive fields of their thalamic inputs have a concentric on and off organization[1]. This dramatic transformation suggests that there are specific rules governing the connections made between thalamic and cortical neurons[1–3] (see ref. 4). Here we report a study of these rules in which we recorded from thalamic (lateral geniculate nucleus; LGN) and cortical neurons simultaneously and related their receptive fields to their connectivity, as measured by cross-correlation analysis[5,6]. The probability of finding a monosynaptic connection was high when a geniculate receptive field was superimposed anywhere over an elongated simple-cell subregion of the same signature (on or off). However, 'inappropriate' connections from geniculate cells

of the opposite receptive field signature were extremely rare. Together, these findings imply that the outline of the elongated, simple receptive field, and thus of cortical orientation selectivity, is laid down at the level of the first synapse from the thalamic afferents.

Spatiotemporal white-noise stimuli[7,8] (random checkerboards) were used to make detailed maps of the receptive fields of neurons recorded simultaneously in the lateral geniculate nucleus and the cortex. Figure 1 shows an example from such a dual recording. The geniculate receptive field had a classical on-centre/off-surround organization (Fig. 1*a*) and the cortical simple receptive field was obliquely oriented, with adjacent on and off subregions (Fig. 1*c*). To quantify the degree of overlap, we calculated parameters that corresponded to the position and size of the X-cell receptive field[9] (Fig. 1*b*) and to the position, orientation, length and width of the simple-cell subregions[10] (Fig. 1*d*). The on centre of the geniculate neuron (red circle) had a high degree of overlap with the on subregion of the simple cell, as can be seen in both the raw data (Fig. 1*c*) and the smoothed model receptive field (Fig. 1*d*).

Independent of the receptive-field measurements, cross-correlation analysis provided a quantitative test for direct monosynaptic connections between simultaneously recorded geniculate and cortical cells. As has been shown in a similar study[11,12], positive cross-correlations between LGN and cortical neurons show features that are consistent with monosynaptic connections: fast latencies and rise times, both of around 1–2 ms. The criterion we used for a monosynaptic connection was that the cortical neuron was significantly more likely to fire between 1 and 4.5 ms after a geniculate spike. For example, the neurons whose receptive fields are illustrated in Fig. 1 were strongly correlated at this very fast time scale (Fig. 2*a*). The fraction of cortical spikes accounted for by this 'monosynaptic' peak[11,12] (the strength of the correlation) was 7.8% in this example. When the slow events were removed from the cross-correlation (Fig. 2*b*) the fast monosynaptic peak was found to be highly significant ($P < 10^{-6}$). The statistical test was performed on these 'filtered' data, but the strength of connection was measured by subtracting the baseline from the unfiltered cross-correlations (this method is similar to a shuffle-subtraction[13]).

TABLE 1 Connections between overlapping X cells and simple cells

	Connected	Total	Percentage	Strength mean/median (%)
Same-sign	17	27	63%	3.5/2.6
(centred)	6	7	86%	2.1/1.6
Border	5	31	19%	2.4/2.0
Opposite-sign	1	16	6%	0.2/0.2
Total	23	74	31%	3.1/2.4

Summary of connected geniculate/simple-cell pairs as a function of receptive-field overlap. Geniculate X cells were divided into three categories according to the position of their receptive fields relative to the nearest simple cell subregion. If the X-centre was within the central 50% of a simple subregion (along its width) and had the same response signature (on or off) then it was called same-sign. The opposite-sign category was defined similarly, but for the opposite response signature. Otherwise the X cell was said to be along a border of a simple subregion. Most (17 of 27) of the same-sign cells were connected, but only one of 16 opposite-sign cells was. Same-sign geniculate cells were also said to be centred if they were over the strongest simple subregion (as opposed to a weaker flank), within half a standard deviation of the peak along its length, and within the central 40% in width. Of the 7 centred geniculate cells, 6 were connected. The last column shows both the mean and median strengths (see Fig. 2*b*) of the positive correlations in each category. Because of correlations between thalamic neurons themselves, these values may be overestimates of the connection strengths between thalamic and cortical neurons[15].

One potential problem was that cells with the opposite response signature (for example, an off geniculate neuron superimposed with an on simple subregion) were less likely to be co-activated by the visual stimulus. Because the visual stimuli created a negative correlation between the cells' firing on a long

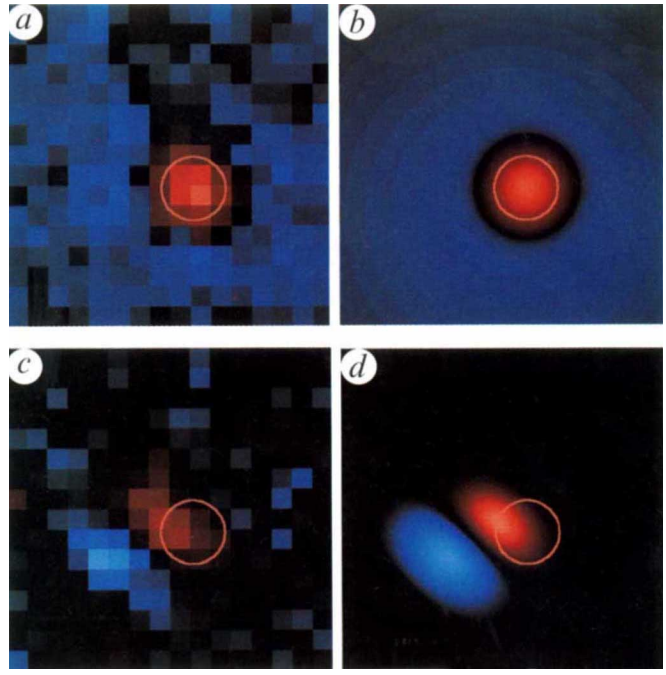

FIG. 1 Receptive field maps of a geniculate X cell (*a*) and simple cell (*c*). Hue codes for response sign (red for on responses, blue for off), and brightness codes for response strength. The geniculate cell (*a*) was on-centre/off-surround: the region in the centre corresponds to the area where the neuron was excited by a light stimulus; the brighter the red, the stronger the excitation. The diffuse blue region (the surround) corresponds to an area where it was weakly excited by a dark stimulus. Black corresponds to areas where the neuron was indifferent to light and dark stimuli. The cortical receptive field (*c*) has elongated on and off subregions. In *b* and *d*, these receptive field maps are fitted to functional forms: a difference of gaussians[9] for the geniculate cell, and a Gabor function[10] for the cortical cell. The centre region of the geniculate cell is marked by a red circle with a radius of 1.5 standard deviations of the centre gaussian. This centre is reproduced on all maps to show the degree of overlap of the two receptive fields.
METHODS. Cats were anaesthetized with ketamine (10 mg per kg, intramuscular) and sodium pentothal (2 mg per kg per h), followed by paralysis with recuronium bromide (0.2 mg h^{-1}, intravenous). Temperature, electrocardiogram, electroencephalogram and expired CO_2 were monitored continuously throughout the experiment. Eyes were dilated with 1% atropine and the nictitating membrane retracted with 10% phenylephrine. The refractive error was measured with a slit ophthalmoscope and corrected with clear contact lenses of the appropriate curvature. Action potentials of single neurons in both the geniculate and area 17 were recorded with plastic-coated tungsten microelectrodes, and were collected on a personal computer running Brainwave software (Broomfield, CO). Receptive-field eccentricities ranged between 5° and 10°. Often, two neurons were recorded simultaneously on either the geniculate or cortical electrode. Visual stimuli were created with a personal computer video-graphics card (Pepper Graphics System, Number Nine Computer Corporation) and presented on a cathode ray tube monitor (NEC Multisync). The white-noise stimulus consisted of a 16 by 16 grid of square pixels. For every frame of the stimulus, each pixel was either black or white according to a binary temporal signal, known as a maximal-length shift register sequence, or m-sequence[7,14]. The stimulus was updated every two frames of the 100 Hz or 80 Hz video display (every 20 or 25 ms). A complete m-sequence had $2^{15}-1=32{,}767$ frames and lasted 11 min. The pixel size was 0.4° in most cases, including the data illustrated, and the entire stimulus spanned 6.4°. The receptive-field map is defined as the average stimulus that preceded each action potential as a function of the delay; it is the spatial stimulus that tended to make the neuron fire[7,8].

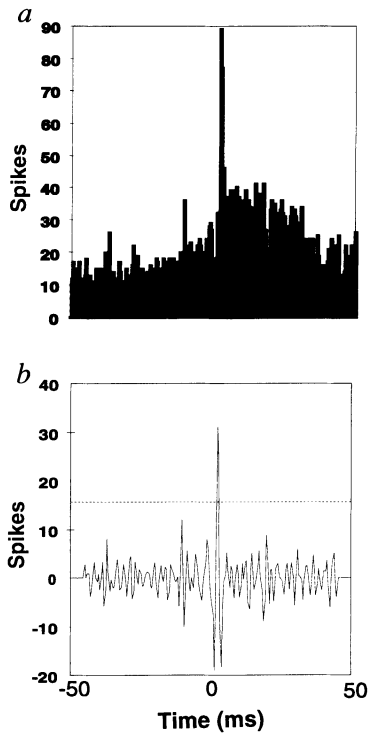

FIG. 2 Cross-correlation between the geniculate and cortical neurons illustrated in Fig. 1. The ordinate gives the number of times the cortical neuron fired as a function of the delay between geniculate and cortical firing (+50 ms, in steps of 0.5 ms). The cortical cell was most likely to fire between 1 and 4.5 ms after a geniculate action potential. The strength of a connection or the contribution[10,11]—the percentage of the cortical spikes that were accounted for by the 'monosynaptic' peak (1–4.5 ms) above the baseline—was 7.8%. Data were collected over 11 min during white-noise stimulation. Geniculate spikes, 9,740; cortical spikes, 2,176. The baseline was defined as the total number of spikes between −4.5 and −1.0 ms. To minimize false negatives, only cross-correlations that had a baseline of >50 spikes were included. This value was chosen because, of the 15 cross-correlations that had <50 spikes (not included in our sample), only one had a statistically significant peak, whereas 5 of the 12 cross-correlations with baselines between 50 and 100 had significant peaks. Cross-correlations were calculated from periods of visual stimulation either with white noise (12 positive out of 37), or with oriented gratings (11 positive out of 37). For the grating data, the strengths calculated from the shuffle-subtractions[13] (average 2.0, median 1.4) and with the subtraction of the baseline (average 1.6, median 1.8) were very similar. *b*, Test of statistical significance. The same cross-correlation was bandpass filtered between 75 and 700 Hz to capture only the fastest, 'monosynaptic' correlations. These frequencies are faster than most visual responses, so this procedure removed stimulus-dependent correlations just as effectively as a shuffle-subtraction. The broken line indicates the significance level set at a probability of 0.2%, assuming a normal distribution. As there are eight samples in the range 1–4.5 ms, this corresponds to a probability of $P<1.6\%$. This criterion was used for all of the cross-correlations in the study.

time scale (>10 ms), there was occasionally very little baseline on which to observe a 'monosynaptic peak' in the cross-correlation. This problem was less severe with the white-noise input than with drifting gratings, because cells were less dominated by any single feature of the stimulus. Nevertheless, to minimize false negatives we rejected cell pairs whose cross-correlations had very few spikes in the baseline (for both white-noise and grating stimuli, see Fig. 2 legend). This ensured that the two neurons were co-active on a slow, visually evoked time scale frequently enough for a fast monosynaptic influence to be detected.

We recorded from 104 superimposed pairs of geniculate and simple cells for long enough to characterize their receptive fields and to collect cross-correlations with an adequate baseline (Fig. 2*a*). Here we consider those 74 pairs for which the geniculate cells were X cells with centres similar in size to the cortical subfields. Of these 74 X cells, 23 were positively correlated with a superimposed simple cell ($P<0.016$; see Fig. 2*b*). The strength of the positive correlations ranged from 0.2% to 10.3%, with an average of 3.1%. For the remaining 30 pairs the geniculate cells had larger receptive fields and were probably Y cells. Eight of these 30 cells were positively correlated with a simple cell[11,12], but there was no clear relation between receptive-field overlap and the probability of connection. These cells will not be considered further in this study.

The mapping techniques used here allowed us to extend previous results[11,12] by relating the receptive-field positions of the geniculate and cortical neurons to the probability of finding a connection between them. Ideally, we would record from all the geniculate cells whose receptive fields overlap a single simple cell. Instead, data collected from different simple-cell/X-cell pairs were compared by using their functional forms (Fig. 1*b*, *d*), which were rotated and stretched onto an idealized receptive field (Fig. 3). If the strongest simple subregion was off, the signs of the cortical and geniculate receptive fields were inverted. The 74 X cells were densely scattered over the model simple receptive field. In Fig. 3 we show just the 23 X cells that were positively correlated. The size of the circles represents the X-cell centre, the colour represents the signature relative to the central, strongest cortical subregion (red, same sign; blue, opposite sign), and the thickness represents the strength of the correlation.

The centres of most of the connected geniculate neurons were well superimposed with a simple cell subregion of the same sign. This demonstrates that individual simple cells receive input from both on and off geniculate cells whose centres are aligned along the axis of each subregion.

To tabulate the probability of finding a monosynaptic connection, cell pairs were grouped according to the spatial overlap between the geniculate centre and the nearest cortical subregion. The percentage of positively correlated pairs was calculated for

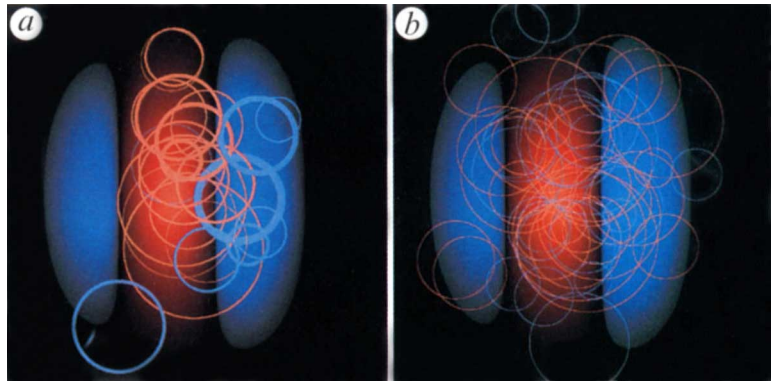

FIG. 3 Summary of the spatial relation between simple and geniculate receptive fields of the 23 functionally connected cell pairs (those with positive correlations). The receptive field fitted for each simple cell was transformed (rotated and stretched) into an idealized receptive field. The geniculate centres are shown in relation to the idealized simple cell, which has a strong subregion in the centre (red) and two flanks of unequal strength (blue). Geniculate centres with the same sign as the strongest simple subregion are shown in red, those with the same sign as the flanks in blue. The diameter indicates the relative receptive-field size (1.5 standard deviations), and thickness indicates the strength of the correlation, from 0.2% to 10.3%. *b*, Spatial relation between simple and geniculate receptive fields of the 51 pairs that were not functionally connected.

three groups: opposite-sign, border and same-sign (Table 1). Most (17 of 27) of the same-sign geniculate cells were connected, as would be expected according to the original Hubel and Wiesel model[1]. A small fraction of the border cells (5 of 31) had positive correlations, but only one of the opposite-sign geniculate cells in our sample was connected. The strength of this 'inappropriate' connection was the weakest seen, only 0.2%. There was no other association between receptive-field overlap (for example, same-sign versus border) and the strength of the positive correlations.

Because a significant fraction of the same-sign cells were not connected, we examined several subcategories to see if any had a higher probability of being connected. There was no asymmetry between on and off; in particular, off-centre X cells were connected to simple cells whose strongest subregion was off and to simple cells with off flanks. An almost equal percentage of the same-sign cells that were over the strongest subregion were connected (12 of 20) compared to those over a flank (5 of 7). However, of the same-sign X cells that were over the strongest subregion, those that were very well centred in length and width had the highest proportion of positive correlations (6 of 7).

In summary, the connections made between geniculate X cells and simple cells were very specific. If the geniculate receptive field centre overlapped an appropriately signed simple subregion, the probability of connection was high (63%). The probability was highest if the X cell was well centred over the strongest simple subregion (86%), and decreased in both width and length. There were very few exceptions to these simple rules: only one of the 23 connected X cells was superimposed with a subregion of the wrong response sign. Thus both the subfield organization and the orientation of simple receptive fields are well established by the monosynaptic thalamic inputs. These findings imply specificity at the finest level, not only in terms of the afferents that project to a given column[2], but also in terms of the selective connections made with different cortical neurons within a column. The specificity of the thalamocortical projection does not deny a role for intracortical connections, both excitatory and inhibitory, in strengthening orientation selectivity. It does, however, demonstrate the importance of the geniculate input in the creation of simple receptive fields. □

Received 16 June; accepted 3 October 1995.

1. Hubel, D. H. & Wiesel, T. N. *J. Physiol., Lond.* **160,** 106–154 (1962).
2. Chapman, B., Zahs, K. R. & Stryker, M. P. *J. Neurosci.* **11,** 1347–1358 (1991).
3. Ferster, D. *J. Neurosci.* **7,** 1780–1791 (1987).
4. Sillito, A. M. *J. Physiol., Lond.* **250,** 305–329 (1975).
5. Alonso, J. M., Reid, R. C. & Wiesel, T. N. *Soc. Neurosci. Abstr.* **19,** 425 (1993).
6. Reid, R. C., Alonso, J. M. & Wiesel, T. N. *Soc. Neurosci. Abstr.* **20,** 425 (1994).
7. Reid, R. C. & Shapley, R. M. *Nature* **356,** 716–718 (1992).
8. Jones, J. P. & Palmer, L. A. *J. Neurophysiol.* **58,** 1187–1211 (1987).
9. Rodieck, R. W. *Vision Res.* **5,** 583–601 (1965).
10. Jones, J. P. & Palmer, L. A. *J. Neurophysiol.* **58,** 1233–1258 (1987).
11. Tanaka, K. *J. Neurophysiol.* **49,** 1303–1318 (1983).
12. Tanaka, K. *Vision Res.* **25,** 357–364 (1985).
13. Perkel, D. H., Gerstein, G. L. & Moore, G. P. *Biophys. J.* **7,** 419–440 (1967).
14. Sutter, E. *Adv. Meth. Physiol. Systems Model.* **1,** 303–315 (Univ. Southern California, 1987).
15. Usrey, W. M., Alonso, J. M. & Reid, R. C. *Soc. Neurosci. Abstr.* **21,** 21 (1995).

ACKNOWLEDGEMENTS. Both authors contributed equally to this work. We thank T. N. Wiesel for discussion, J. Hirsch for comments on the manuscript, W. M. Usrey for help with some of the experiments, and C. Gallagher and K. McGowan for technical assistance. This study was supported by the NIH, the Klingenstein Fund, Fulbright/MEC, and the Charles H. Revson Foundation.

Displacement of corticotropin releasing factor from its binding protein as a possible treatment for Alzheimer's disease

Dominic P. Behan*, Stephen C. Heinrichs*, Juan C. Troncoso†‡, Xin-Jun Liu*, Claudia H. Kawas‡, Nicholas Ling* & Errol B. De Souza*§

* Neurocrine Biosciences, Inc., 3050 Science Park Road, San Diego, California 92121, USA
Neuropathology Laboratory, Departments of † Pathology and ‡ Neurology, Johns Hopkins University School of Medicine, Baltimore, Maryland 21205, USA

In Alzheimer's disease (AD) there are dramatic reductions in the content of corticotropin releasing factor (CRF)[1–4], reciprocal increases in CRF receptors[1,2], and morphological abnormalities in CRF neurons[5] in affected brain areas. Cognitive impairment in AD patients is associated with a lower cerebrospinal fluid concentration of CRF[6], which is known to induce increases in learning and memory in rodents[7–9]. This suggests that CRF deficits contribute to cognitive impairment. The identification in post-mortem brain of CRF-binding protein (CRF-BP)[10,11], a high-affinity binding protein that inactivates CRF, and the differential distribution of CRF-BP[12] and CRF receptors[13], provides the potential for improving learning and memory without stress effects of CRF receptor agonists[14]. Here we show that ligands that dissociate CRF from CRF-BP increase brain levels of 'free CRF' in AD to control levels and show cognition-enhancing properties in models of learning and memory in animals without the characteristic stress effects of CRF receptor agonists.

§ To whom correspondence should be addressed.

Previous studies have defined the characteristics and distribution of CRF-BP in rat brain[12], sheep brain[10] and human plasma[15–17]. Our initial studies focused on the identification and characterization of CRF-BP in post-mortem human brain. Brains were obtained post-mortem from ten demented individuals (NINCDS clinical diagnosis criteria[18]) with pathologically confirmed AD (NINCDS pathological diagnosis criteria[19]) (7 males and 3 females; age 74 ± 3.5 years (range 59–89 years); post-mortem delay 6.9 ± 0.7 h (range 3–12 h) and ten age-matched neurologically normal controls (2 males and 8 females; age 76 ± 3.1 years (range 52–85 years); post-mortem delay 6.9 ± 0.6 h (range 5–10 h)). All AD cases showed abundant amyloid deposits, neuritic plaques and variable densities of neurofibrillary tangles in neocortex, fulfilling NINCDS criteria[19]. The control cases showed no evidence of neocortical pathology. Most of the CRF-BP-like immunoreactivity (CRF-BP-IR) (>85%) in human cerebral cortex was membrane associated as a result of the presence of activity in the membrane pellets after centrifugation of the tissue extracts. These data are in accordance with studies in sheep-brain homogenates[10] and in slide-mounted sections of rat brain[12], demonstrating a predominantly membrane/neuronal localization of the CRF-BP. The membrane-associated form of the CRF-BP in human brain has pharmacological characteristics similar to those of the recombinant form of the soluble plasma CRF-BP (Table 1).

The levels of CRF and CRF-BP in the cerebral cortex of Alzheimer's patients and age-matched controls were then compared. In agreement with previous observations[1–4], there were dramatic reductions in the concentration of CRF-IR in the frontal, parietal and temporal cerebral cortex, with a tendency for a non-significant decrease in occipital cortex (Fig. 1*a*). Conversely, there were no significant differences seen in CRF-BP-IR in any of the four cerebrocortical areas examined in AD, regardless of whether the CRF-BP was assayed using a ligand immunoradiometric assay or enzyme-linked immunosorbent assay (ELISA) (Fig. 1*b*). Furthermore, the pharmacological profile of the CRF-BP in AD tissue was similar to that previously described for age-matched controls and the recombinant form of CRF-BP (Table 1). These data provide evidence for the